Clays and Clay Minerals, Vol. 35, No. 1, 43–52, 1987.

AUTHIGENIC CHRYSOTILE FORMATION IN THE MATRIX OF QUATERNARY DEBRIS FLOWS, NORTHERN SOUTHLAND, NEW ZEALAND

D. CRAW, C. A. LANDIS, AND P. I. KELSEY[1]

Geology Department, University of Otago
P.O. Box 56, Dunedin, New Zealand

Abstract—Quaternary debris flows derived from ophiolite melange in northern Southland, New Zealand, are locally cemented and veined by cross-fiber and fine-grained chrysotile. Chrysotile was identified by optical, X-ray powder diffraction, electron microprobe, differential thermal (DTA), and infrared analysis methods. Microprobe and DTA also suggested the presence of as much as 6% of sub-microscopic, noncrystalline alumina, probably in the form of pseudoboehmite. Cavity fillings and irregular veins containing chrysotile are as thick as 40 cm and commonly contain lizardite clasts. Calcite commonly accompanies chrysotile as a vein mineral. Magnetite and pyrite are found near and adjacent to chrysotile veins. These accessory minerals imply that the chrysotile formed under alkaline, reducing conditions. Surface water seepages have pH = 9. Remnant debris-flow topography, Holocene radiocarbon dates, and the absence of hot spring activity confirms that chrysotile can form under near-surface, low-temperature conditions. Growth of chrysotile fibers on a lizardite substrate suggests that the chrysotile formed by solution of detrital lizardite and subsequent precipitation in cavities within the debris flow.

Key Words—Authigenesis, Chrysotile, Debris flow, Pseudoboehmite, Serpentine.

INTRODUCTION

The formation of serpentine at low temperature near the Earth's surface has been suggested by several authors (e.g., Cashman and Whetten, 1976; Barnes and O'Neill, 1969; Barnes *et al.*, 1978; Wenner and Taylor, 1973; Neal and Stanger, 1984). No unequivocal geological evidence, however, for surficial authigenic serpentine growth has been reported. This study describes occurrences of chrysotile, including some coarsely asbestiform material, found cementing and veining Quaternary debris flows in Southland, New Zealand.

GENERAL GEOLOGY

In western Southland deeply incised, U-shaped glacial valleys have been cut into mafic and ultramafic rocks of the Dun Mountain ophiolite belt and the overlying late Paleozoic clastic sediments and limestones of the Maitai Group (Coombs *et al.*, 1976). Since retreat of the Quaternary glaciers about 14,000 years ago (McKellar, 1973; Suggate, 1965), many oversteepened valley walls have collapsed. Spectacular debris flows, as long as 4 km, have been derived from the rocks in the Dun Mountain ophiolite belt (Figure 1). These debris-flow deposits and associated talus cones consist of crudely stratified, moderately indurated breccias as thick as 50 m (Figure 2). They contain serpentinite, partly serpentinized peridotite, and gabbroic clasts as large as 5 m in diameter. Breccia matrixes consist mainly of fine-grained serpentinite and mafic detritus which is locally cemented by authigenic minerals.

Authigenic calcite, aragonite, stevensite, pectolite, and pyroaurite in the form of cement, veins, and clast coatings in the Acheron debris flow (Figure 1) were described by Craw and Landis (1980). In that study, the apparent absence of authigenic serpentine was noted. Further work on this debris flow and a similar debris flow in the east Eglinton River (Figures 1 and 2), however, has revealed that chrysotile veins are indeed present. The following data and discussions are intended to show that this serpentine formed under essentially surficial conditions.

CHRYSOTILE LOCALITIES

Acheron Stream

Pale-green chrysotile occurs as an authigenic filling in veins as wide as 2 cm cross-cutting the debris-flow matrix (Figure 3). Veins are continuous for 5–30 cm. In addition, fine-grained chrysotile is commonly found as a cement, coating breccia clasts, and filling fractures in clasts (Figure 3b). At the millimeter scale veins are composite, consisting of zones of relatively coarse, asbestiform chrysotile alternating with zones of finer-grained chrysotile (Figure 4). Cross-fiber and slip-fiber chrysotile coexist in these veins. The matrix of the breccia consists of fine-grained ($\leq$2 mm) serpentinized peridotite fragments. Relict bastite and mesh-serpentine textures are common in larger fragments. Textures and optical properties suggest that most of the non-asbestiform serpentine is lizardite (see Wicks and Whittaker, 1977). Some chrysotile veins are restricted

[1] Present address: Department of Geology, University of Canterbury, Christchurch, New Zealand.

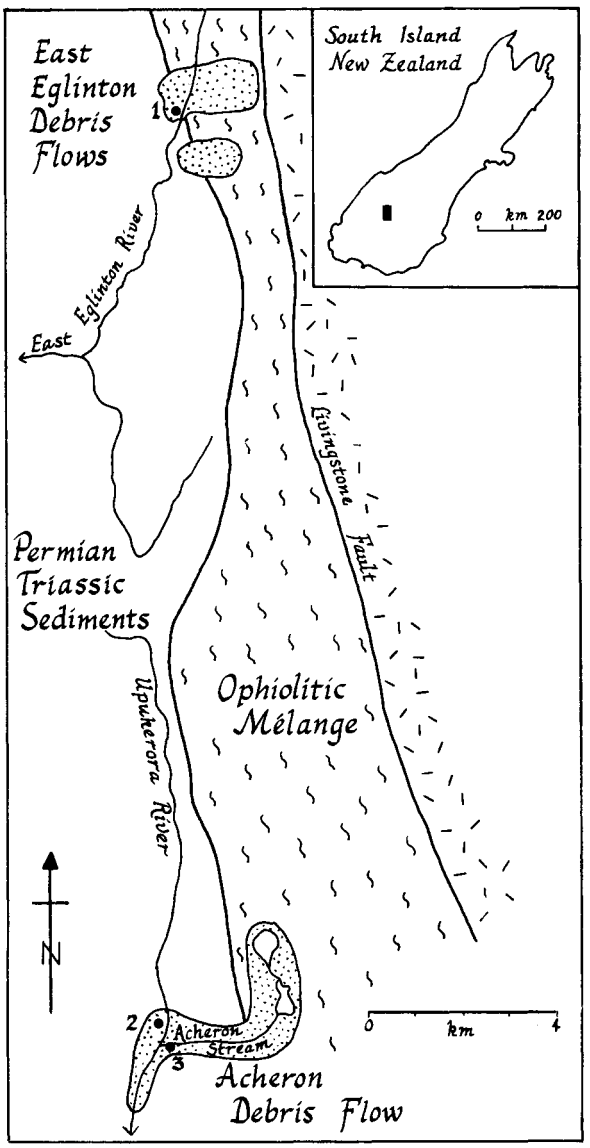

Figure 1. Locality map of the Eglinton-Upukerora area, Southland, New Zealand, showing the debris flows (stippled) derived from ophiolitic melange. Numbers refer to sample localities discussed in text. Caples terrane (metagreywacke and metavolcanics) lies east of the Livingstone Fault (Coombs *et al.*, 1976).

to single lizardite-rich fragments. Thus, unlike the veins and coatings described above, the timing of formation of these veins is equivocal: they formed either *in situ* in the Dun Mountain ophiolite belt after lizardite formation and were rafted down with the debris flow, or they formed after emplacement of the debris flow along with the cross-cutting chrysotile described above.

Magnetite and pyrite are common accessory minerals in clasts and matrix and adjacent to chrysotile vein walls. These opaque minerals show no signs of oxidation within the debris flow. No unequivocally authigenic occurrences of opaque minerals were observed.

Chrysotile fibers are well-formed and euhedral at all scales from hand specimen to electron microscope images (Figure 5). The fibers are characteristically curved at the millimeter scale and show undulose extinction. Refractive indices of fiber bundles ($\gamma = 1.552 \pm 0.003$, $\alpha = 1.540 \pm 0.003$) are consistent with published values for chrysotile (e.g., Chernosky, 1975).

Carbon-14 age determinations of the Acheron debris flow (Table 1) suggest that the deposit formed less than 7000 years ago and that cementation occurred since then. The carbonate cement ages almost certainly reflect an average of progressive cementation from the time of debris-flow formation to the present day.

The debris flow deposits have not been buried, except by local accumulations (<20 m) of late Pleistocene-Holocene fluvial gravels, and there are no hot springs in the region. Hence, authigenic minerals in these deposits must have formed under essentially surficial conditions.

Upukerora River

The authigenic chrysotile at this locality is fine grained and mixed with calcite. In sample OU 45969 these minerals form a pale-green coating on the surface of a highly fractured microgabbro clast. Fractures are filled with a mixture of chrysotile and calcite. Individual fibers of chrysotile are not visible in hand specimen or under the petrographic microscope; however, transmission electron microscope (TEM) images (Figure 5c) show the characteristic elongate crystal morphology.

Eglinton River

Irregular veins (as wide as 40 cm) of fine-grained chrysotile cross-cut the debris flow at this locality. Individual veins are traceable for as far as 3 m. In hand specimen the chrysotile veins are extremely fine grained and waxy, and have a conchoidal fracture. Their color ranges from very pale blue (5B 8/2) to yellowish gray (5Y 7/2) on drying. Scanning electron micrographs (SEM) yielded little information due to the extremely fine grain size of this material, however, tubular fibers were visible by TEM (Figure 5b). Minor calcite is also present.

RESULTS

X-ray powder diffraction (XRD) results

XRD data for material from the three localities described above are presented in Table 2. Glycolation and intersalation with potassium acetate produced no change in the XRD patterns. It is evident from these data that the samples consist almost entirely of serpentine-group minerals. Although the data are somewhat equivocal, they imply the presence of either a clinochrysotile-lizardite mixture or perhaps an or-

https://doi.org/10.1346/CCMN.1987.0350106 Published online by Cambridge University Press

Figure 2. Photographs of cemented debris flow material, in outcrop at East Eglinton River: left = steep cliffs of crudely stratified deposits (person in lower left for scale); right = angular blocks of ultramafic debris cemented by carbonates and chrysotile (pack is 60 cm tall).

thochrysotile-clinochrysotile mix (Table 2). The tubular morphology shown in Figure 5 confirms the identification of chrysotile in the breccia cements. Considering the rarity of orthochrysotile and the common occurrence of lizardite associated with the vein chrysotile, a mixture of clinochrysotile and lizardite seems the more likely interpretation of the XRD data.

Chemistry

Electron microprobe analyses of chrysotile from the three localities are presented in Table 3 and plotted on an Mg-Fe-Al ternary composition diagram in Figure 6. Because ferrous/ferric iron ratio cannot be determined by microprobe, the iron is assumed to be Fe^{2+} in Figure 6 and Table 3, with the exception of a very small amount of Fe^{3+} inferred to make up a tetrahedral site occupancy of 4 (Table 3).

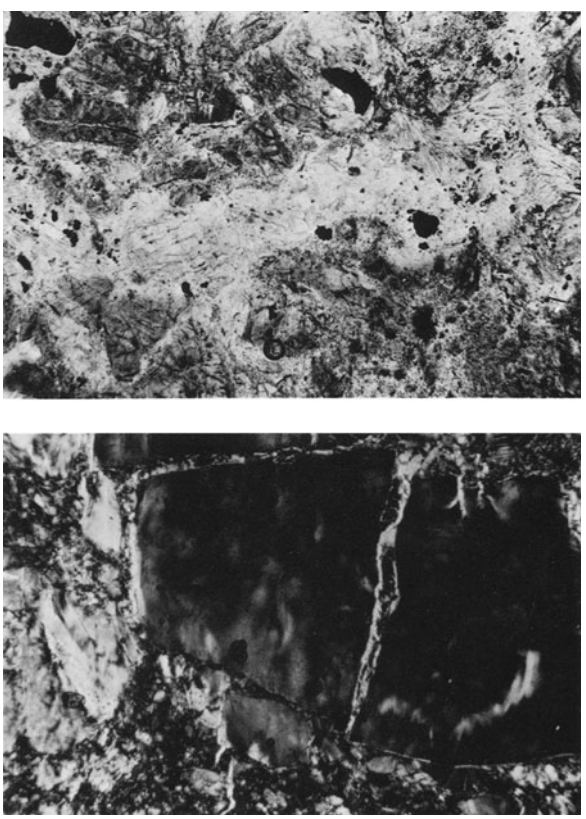

→

Figure 3. Photomicrographs of sample OU 45968 from the Acheron debris flow. Upper = veins of cross-fiber chrysotile (light-colored) cross-cut and cement breccia clasts (dark). Opaque minerals are magnetite (in clasts) and a Ti-oxide (in clasts and veins). Plane polarized light; horizontal field of view = 2.4 mm. Lower = fractured lizardite clast (dark) which has been coated and veined by slip-fiber and cross-fiber chrysotile (white rim on clast fragments). Crossed polars; horizontal field of view = 4 mm.

https://doi.org/10.1346/CCMN.1987.0350106 Published online by Cambridge University Press

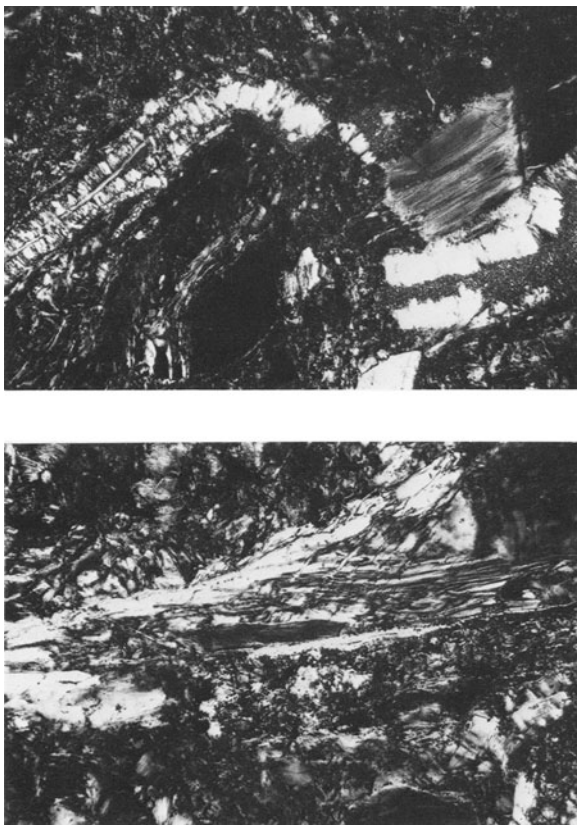

Figure 4. Photomicrographs of chrysotile veins in sample OU 45968, Acheron debris flow. Upper = coarse, fibrous cross-fiber chrysotile vein (light color, left) and composite cross-fiber and irregularly oriented fine-grained chrysotile vein (light color, right) cross-cut breccia matrix. Coarse-grained cross-fiber chrysotile clusters are visible at lower right. Crossed polars; horizontal field of view = 4 mm. Lower = composite cross-fiber, slip-fiber and fine-grained, poorly oriented chrysotile veins crossing breccia matrix. Coarse-grained cross-fiber chrysotile clusters are visible at lower right. Crossed polars; horizontal field of view = 4 mm.

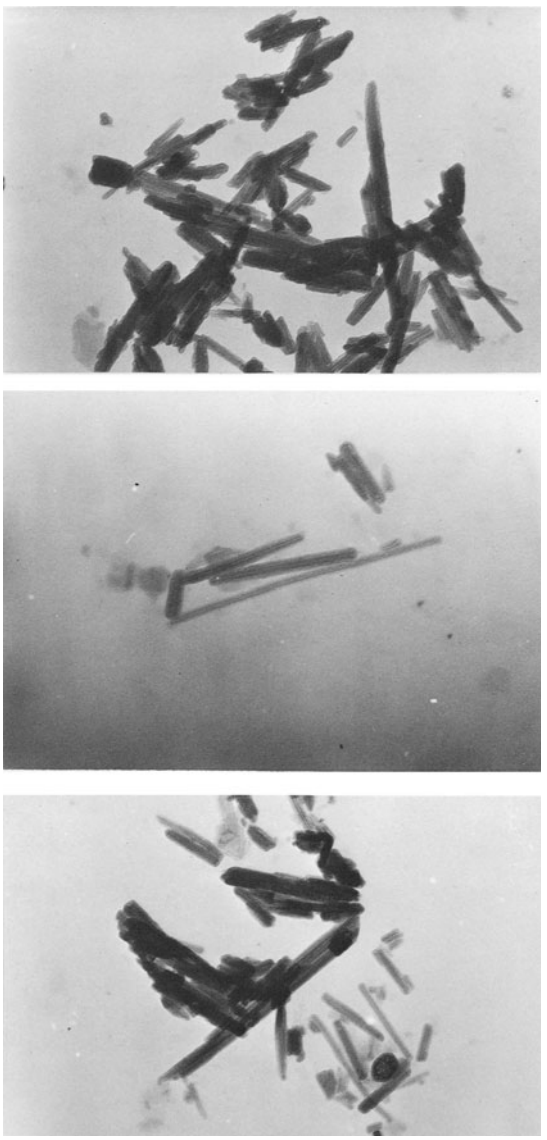

Figure 5. Transmission electron micrographs of dispersed chrysotile fibers from debris flow cements. Upper = sample OU 45968, from Acheron Stream; horizontal field of view = 3 μm. Middle = sample OU 37870 from East Branch, Eglinton River; horizontal field of view = 2 μm. Lower = sample OU 45969 from Upukerora River; horizontal field of view = 3 μm.

Low microprobe anhydrous totals and correspondingly high H_2O contents (determined by loss on ignition) in analyses D and E suggest that the analyzed material contained excess molecular water. This excess may be due to impurities in the samples (see below). Temperatures at which water is lost from the material are indicated in DTA thermograms (see below).

It is apparent from Figure 6 that the chrysotile has a higher Mg/(Mg + Fe) than either clast lizardite from the debris flow or the lizardite from ophiolite outcrops at the debris-flow source. The Al content of the coarse-grained asbestiform chrysotile from Acheron Stream debris flow is low (0.78 wt. % Al_2O_3) and comparable to literature values, which are characteristically less than 1% (e.g., Wicks and Plant, 1979). The Al content of chrysotile-bearing samples from the other two localities, especially the Eglinton material, is higher than previously described chrysotile (Table 3, column E). Small amounts of Al can be accommodated in the chrysotile structure, particularly at high temperatures (Chernosky, 1975), but aluminous serpentine generally has the platy lizardite or antigorite structure. The high (1.8–5.2%) alumina content of the Eglinton material is incompatible with published analyses of chrysotile (cf. Wicks and Plant, 1979); hence a separate aluminous phase intermixed with the Eglinton and possibly the Upukerora chrysotile tubes, may be present. Detailed

https://doi.org/10.1346/CCMN.1987.0350106 Published online by Cambridge University Press

Table 1. Radiocarbon dates, Acheron debris flow, Southland, New Zealand.

Specimen	N.Z. 14C No.[1]	Specimen	Age (yr)
D42/f73	5245 A	Wood from debris flow	6630 ± 100
D42/f74	5246 A	Wood from debris flow	6810 ± 100
D42/f75	5247 A	Carbonate cement	5660 ± 100
D42/f76	5248 A	Carbonate cement	4760 ± 70

[1] New Zealand radiocarbon date number.

scanning of the samples with a 2-μm microprobe beam failed to indicate any inhomogeneity with respect to Si, Al, Mg, or Fe at the micrometer scale. The analyses plotted in Figure 6; however, indicate an alumina enrichment trend joining the Al-poor Acheron and the Al-rich Eglinton material, but no change in the Mg:Fe ratio. This enrichment trend suggests the presence of a separate aluminous phase. The high water contents inferred from loss-on-ignition data (Table 3) imply a hydrous nature for this aluminous phase.

Differential thermal analysis results

DTA curves for chrysotile samples are presented in Figure 7. The overall shapes of portions of these curves, especially that of the Acheron chrysotile, correspond well with curves for chrysotile presented by Farmer (1974) and McKenzie (1970). Naumann and Dresher (1966) showed that the 800°C exotherm increases in size and sharpness with increasing sample surface area. The curves for our material agree particularly well with the high-surface-area chrysotiles reported by them.

Superimposed on the chrysotile DTA curves of samples from Eglinton and Upukerora localities is a separate pattern having endotherms at about 120°, 240°, 400°–440°, and 780°C. The first three endotherms are possibly due to the presence of a poorly defined aluminous phase, possibly pseudoboehmite (Lahodny-Sarc *et al.*, 1978, Figure 7). It should be noted, however, that the pseudoboehmite peaks reported by these authors are all at slightly higher temperature than those reported here. Calcite starts to decompose at about 750°C in clay mixtures (Bain and Morgan, 1969). As calcite is known to be present in the breccia cements (Craw and Landis, 1980) and in the sample analyzed (effervescence in acid), the 780°C endotherm on the thermograms probably represents decomposition of minor calcite impurity in the chrysotile samples, with interference from the chrysotile exotherm at 800°C.

The DTA data suggest that the bulk of the samples is chrysotile and/or lizardite, and that minor calcite is present. In addition, samples from the Eglinton and Upukerora localities contain a third phase, provisionally identified as pseudoboehmite. As shown above, these two samples are more aluminous than the Ach-

Table 2. X-ray powder diffraction data for chrysotile, northern Southland, New Zealand.

						Reference data, Brindley and Brown (1980)							
Acheron Stream		Upukerora River		Eglinton River		Clinochrysotile			Mixture: Clino + Ortho		Lizardite		
d (Å)	I	d (Å)	I	d (Å)	I	*hkl*	d (Å)	I	d (Å)	I	*hkl*	d (Å)	I[1]
7.35	100	7.40	100	7.34	100	002	7.36	100	7.36	100	001	7.4	vs
4.5	40	4.5	40	4.5	30	020	4.56	60	4.56	60	020	4.60	s
3.65	60	3.67	70	3.65	70	004	3.66	100	3.66	80	021	3.90	m
2.68	10	2.66	<10	2.70	10	130	2.66	40	2.66	20	002	3.67	s
2.58	10	2.58	30	2.59	10	201	2.594	40	2.604	40	022	2.875	vw
2.55	10	2.55	<10	2.54	10	$20\bar{2}$	2.549	60	2.547	10	200	2.663	mw
2.50	30	2.50	20	2.50	30	202			2.500	60	201	2.505	vs
2.44	20	2.44	20	2.44	20	202	2.456	80	2.451	70	003	2.410	vvw
				2.295	<10	040			2.285	10	040	2.307	vvw
						203	2.282	20			202	2.156	s
				1.965	<10	$20\bar{4}$	2.215	20	2.212	10	042	1.945	vvw
						204	2.096	60	2.093	40	004	1.835	vw
						205			1.972	10	203	1.799	m
						008	1.829	20	1.828	20	310	1.743	mw
						206	1.748	60	1.746	40	311	1.692	vw
1.530	60	1.530	50 (broad)	1.530	60	060	1.536	80	1.531	70	312	1.572	vvw
						00,10	1.465	20	1.464	20	060	1.538	s
				1.315	10 (broad)	$40\bar{2}$	1.317	40	1.319	40	061,024	1.505	s
						402			1.310	40	005	1.462	vw
											062	1.416	m
											400	1.332	w
											401	1.310	ms

[1] vs = very strong, s = strong, ms = medium strong, m = medium, mw = medium weak, w = weak, vw = very weak, vvw = very very weak.

https://doi.org/10.1346/CCMN.1987.0350106 Published online by Cambridge University Press

Table 3. Analyses[1] of chrysotile from northern Southland, New Zealand.

	A	B	C	D	E
SiO_2	41.5	40.9	40.2	40.3	38.0
Al_2O_3	0.78	0.72	1.25	1.81	5.67
TiO_2	b.d.	b.d.	b.d.	b.d.	b.d.
FeO[2]	3.10	3.79	6.04	2.89	1.41
MnO	0.22	b.d.	b.d.	b.d.	b.d.
MgO	41.8	42.0	39.8	37.2	35.9
CaO	0.00	0.00	0.00	0.00	0.26
Na_2O	0.00	0.00	0.00	0.00	0.00
K_2O	0.00	0.00	0.00	0.00	0.00
Cr_2O_3	0.00	0.00	0.00	0.00	0.00
H_2O (LOI)[3]	12.92	—	—	17.21	17.49
Total	100.32	87.41	87.29	99.41	98.73
	Cations per Si_4O_{10} (anhydrous)				
Si	3.89	3.85	3.83		
Al	0.09	0.08	0.14		
Fe^{3+}	0.02	0.07	0.03		
	Σ 4.00	4.00	4.00		
Fe^{2+}	0.22	0.23	0.45		
Mn	0.02	—	—		
Mg	5.84	5.85	5.65		
	Σ 6.08	6.11	6.10		

b.d. = below detection limit. (A) Acheron Stream, asbestiform chrysotile. (B) Acheron Stream, massive chrysotile (anhydrous total). (C) Acheron Stream, lizardite clast (anhydrous total). (D) Upukerora River authigenic serpentine plus probable pseudoboehmite. (E) Eglinton River, authigenic serpentine plus probable pseudoboehmite.

[1] Analyses determined using a JEOL JXA-5A microprobe, 15-kV accelerating voltage, wave-length dispersion system; specimen current = 0.02 A, beam diameter = 10 μm on periclase.

[2] All Fe as Fe^{2+}.

[3] Loss on ignition (LOI) determined with Meeker burner in Pt crucible on about 0.1-g ground sample, after calcite was removed with 10% HCl and sample washed and air-dried. Values are averages of duplicate runs.

eron chrysotile, the DTA pattern of which lacks the three lower temperature endotherms.

Infrared results

The IR spectrum of the Eglinton chrysotile (Figure 8) is similar to that of chrysotile reported by Farmer (1974) and Luce (1971). Minor bands at 1420 and 310 cm^{-1} may represent internal and lattice modes of calcite, respectively (Farmer, 1974). The frequencies of the chrysotile and calcite bands overlap the characteristic bands of poorly crystalline aluminum oxyhydroxide (cf. pseudoboehmite) reported by Lahodny-Sarc *et al.* (1978); hence it is not possible to detect this material by IR.

Pseudoboehmite

The above data suggest the presence of breccia cements of chrysotile containing impurities of calcite and an aluminous phase resembling pseudoboehmite (Lahodny-Sarc *et al.*, 1978) in samples from Eglinton and

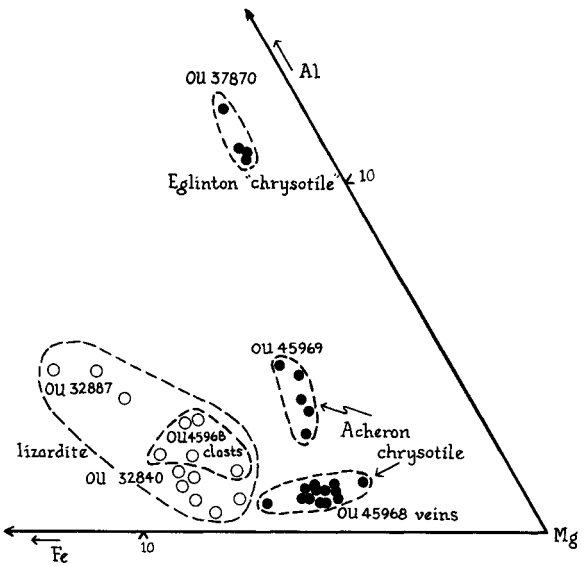

Figure 6. Portion of Al-Fe-Mg composition (atomic proportions) triangle showing the compositions of chrysotile from debris flow matrices and lizardites from debris flow clast (sample OU 45968) and the ophiolite belt source area (samples OU 32887, OU 32840).

Upukerora Rivers. Pseudoboehmite is a poorly defined material with intramicellar structure ranging from noncrystalline to truly crystalline (Papee *et al.*, 1958). The water content is not known to any degree of certainty (Le Bot, 1962), but Yalman *et al.* (1960) suggested that it was in the ratio Al_2O_3:1.3H_2O. XRD peaks for pseudoboehmite are broad and poorly defined, but are in the same position as boehmite peaks (Lahodny-Sarc *et al.*, 1978). Such peaks were not observed in the XRD patterns obtained from samples containing authigenic chrysotile, but the small amount of pseudoboehmite present (<6% as estimated from chemical analyses) would preclude its detection by this technique.

Further evidence for the presence of a pseudoboehmite-like substance in the breccia samples, rather than Al-rich chrysotile (cf. Serdyuchenko, 1945) or crystalline Al-oxyhydroxides, was obtained from refractive index data. Experimental work on formation of Al-rich serpentines by Chernosky (1975) yielded a curve relating Al content to aggregate refractive index. Aggregate refractive index increases with Al content from about 1.55 ± 0.05 (zero Al_2O_3 content) to 1.57 (Al_2O_3 = 18%). The aggregate refractive index for both Al-bearing serpentine samples examined in this study is 1.54, below Chernosky's minimum value; hence the data suggest the absence of Al from the serpentine structure.

Aluminum oxide minerals have been reported coexisting with chrysotile (e.g., Page and Coleman, 1967). All crystalline forms of aluminum oxyhydroxides and oxides, however, have refractive indices greater than 1.55; their presence in the samples would therefore increase the aggregate refractive index. The refractive

https://doi.org/10.1346/CCMN.1987.0350106 Published online by Cambridge University Press

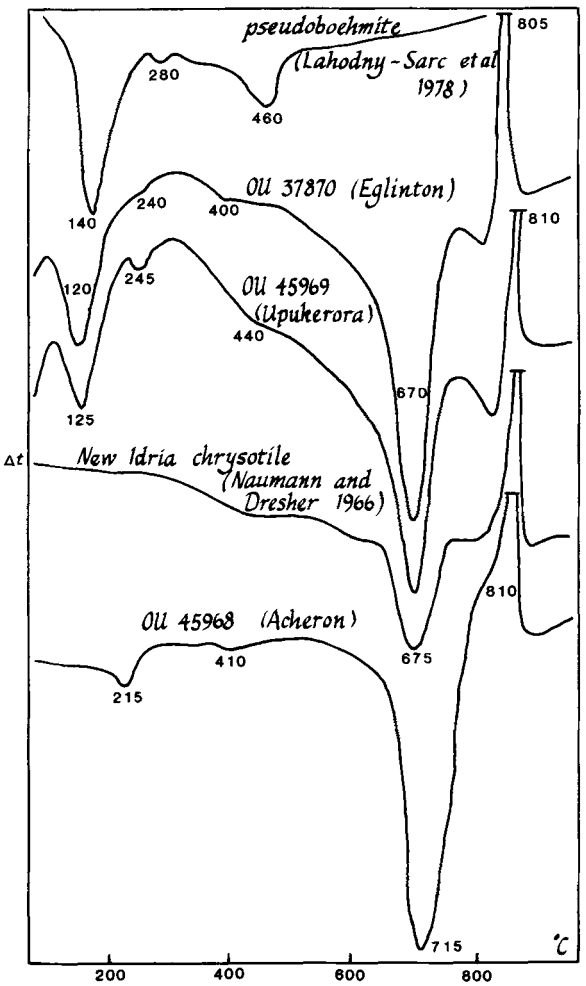

Figure 7. Differential thermal analysis curves for Acheron chrysotile (sample OU 45968) and Eglinton (sample OU 37870) and Upukerora (sample OU 45969) chrysotile-bearing material. Heating rate = 30°C/min. Typical chrysotile (New Idria (Coalinga), California, Naumann and Dresher, 1966) and pseudoboehmite (Lahodny-Sarc *et al.*, 1978) are shown for comparison.

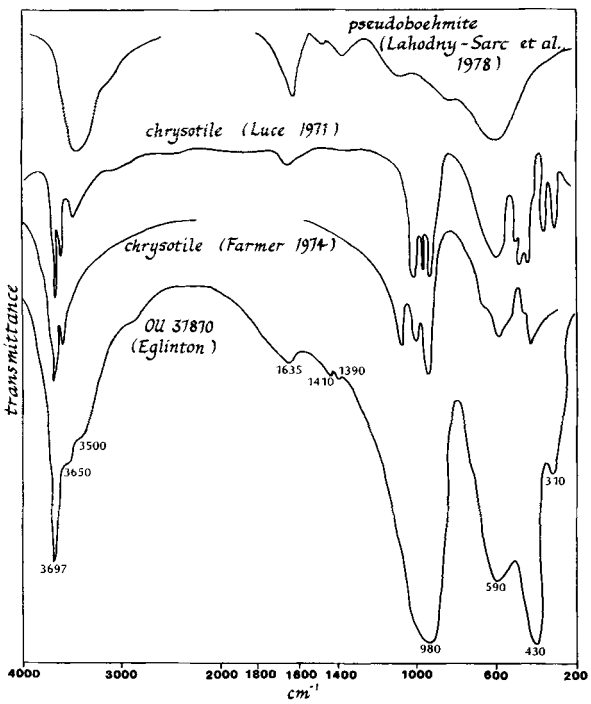

Figure 8. Infrared spectra of chrysotile from Eglinton debris flow (sample OU 37870), other chrysotiles, and pseudoboehmite.

index of pseudoboehmite is not known and may not be constant; however, the loosely bound structure and relatively high water content of pseudoboehmite implies that its refractive indices must be significantly lower than 1.64, the minimum for boehmite in the same manner that the mean index of refraction of kaolinite (n = 1.56) is greater than that of its noncrystalline analogue, allophane (n = 1.48). Thus, a hydrous and poorly crystalline pseudoboehmite-like material may be responsible for the low aggregate refractive index of the Upukerora and Eglinton chrysotile samples.

Fluid composition

Because the geological occurrence of this authigenic serpentine is well understood, constraints can be placed on the chemical conditions under which the material formed. Water in equilibrium with atmospheric CO_2 and calcite (which accompanies the chrysotile) has a pH of 8.4 and a dissolved carbonate concentration (as HCO_3^-) of about 10^{-3} mole/liter (Garrels and Christ, 1965). This pH is in moderately good agreement with the pH of present seepages from the Acheron debris flow (pH = 9, determined with universal pH paper; Craw and Landis, 1980). Magnetite and pyrite in the Acheron debris flow show no signs of oxidation, even those grains that protrude from the matrix into authigenic chrysotile veins. Thus, the chrysotile probably formed under relatively reducing conditions.

Hemley *et al.* (1977) defined relative stability limits for chrysotile and talc with respect to $[Mg^{2+}]$, $[SiO_2(aq)]$, and pH. Inasmuch as stevensite, a common constituent of the Acheron debris flow (Craw and Landis, 1980), probably approximates talc thermodynamically (with additional molecular water), stevensite is used instead of talc in the following discussions (cf. Hemley *et al.*, 1977). From Figure 9, it is apparent that in a solution undersaturated with respect to quartz, chrysotile is stable if $[Mg^{2+}] > 10^{-3}$ at a pH of about 8.4. The value $\log[Mg^{2+}]/[H^{2+}]$ in surficial waters derived from serpentine terrains is in the range 12–20 and commonly exceeds 14 (see Barnes and O'Neill, 1969; Barnes *et al.*, 1978; Cleaves *et al.*, 1974). Hence, the Mg^{2+} content of fluids associated with serpentine terrains is com-

https://doi.org/10.1346/CCMN.1987.0350106 Published online by Cambridge University Press

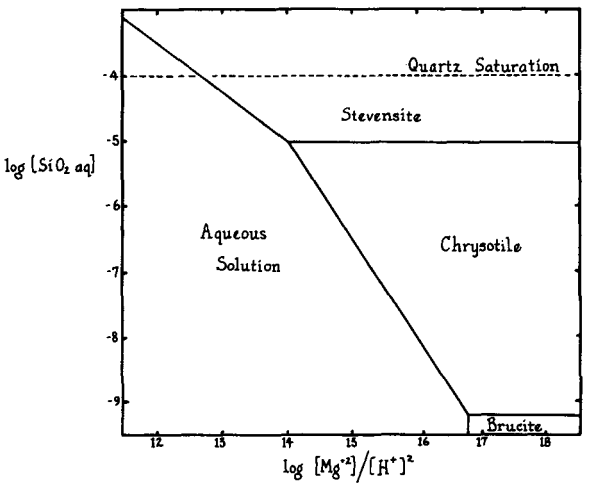

Figure 9. Diagram (after Hemley *et al.*, 1977) showing solubility and phase relationships of brucite, chrysotile, and stevensite with respect to aqueous silica and $[Mg^{2+}]/[H^+]^2$.

monly sufficiently high (at the prevailing pH) for chrysotile formation. Presumably, $[Mg^{2+}]$ exceeded 10^{-3} in the studied debris-flow fluids during chrysotile formation.

Another control on the surficial formation of chrysotile is the aqueous silica content of the fluid. Natural waters in serpentine terrains contain from 10^{-6} to 10^{-4} mole/liter SiO_2 (e.g., see Barnes and O'Neill, 1969; Barnes *et al.*, 1978; Cleaves *et al.*, 1974). This range spans the stability boundary between chrysotile and stevensite (Figure 9). Hence, at a typical Mg^{2+} content for serpentine terrains (see above), stevensite ($[SiO_2(aq)] > 10^{-5}$) should precipitate from high-silica waters, whereas relatively low-silica waters should precipitate chrysotile. Local variations in $SiO_2(aq)$ may thus have produced authigenic stevensite and chrysotile in different parts of the Acheron debris flow. These two minerals have not yet been found coexisting. Under hydrothermal conditions, relatively low silica (at a given Mg^{2+} content) favors serpentine with respect to stevensite (Sakamoto *et al.*, 1981) or sepiolite (Bonatti *et al.*, 1983). Variations in silica content of water percolating through the Acheron debris flow may be related to variations in relative proportions of mafic (relatively high silica) and ultramafic debris. No brucite has been identified in the Acheron debris flow, hence, the fluid aqueous silica concentration must have remained above about $10^{-9.5}$ mole/liter.

DISCUSSION AND CONCLUSIONS

Formation reaction

The above discussion suggests that chrysotile can form under surficial conditions in a high $[Mg^{2+}]$, low-to-moderate $[SiO_2(aq)]$ fluid under alkaline conditions in a relatively reducing environment. The geological occurrences described above suggest that the chrysotile formed from lizardite by solution and re-precipitation (see also, Mumpton and Thompson, 1975; Wicks and Whittaker, 1977; Laurent and Hebert, 1979) rather than from primary peridotite (Barnes and O'Neill, 1969; Barnes *et al.*, 1978). The chrysotile in the samples studied in the present investigation has lower Fe/(Fe + Mg) and inferred lower Al than the parent lizardite, and may coexist with a pseudoboehmite-like material. Hence the formation reaction is probably of the form:

$$\text{Lizardite} \rightarrow Mg^{2+}(aq) + Si^{4+}(aq) + Al^{3+}(aq) + Fe^{2+}(aq) + H_2O \rightarrow \text{chrysotile} + \text{pseudoboehmite}.$$

Additional Al may have been supplied by the dissolution of other material in the debris flow, e.g., gabbro clasts.

Slip-fiber chrysotile formation

The formation of slip-fiber chrysotile asbestos has commonly been related to shearing during serpentinization (e.g., Wicks and Whittaker, 1977). While this relationship may hold in most deposits, it is not clear whether this is so in the Acheron debris flow, as this debris flow has not undergone significant shearing since it formed. Internal shearing, either during debris-flow emplacement or during post-depositional downslope drag (Postma, 1984), may have produced discontinuous zones of high permeability where ground-water-induced vein development was localized. Authigenic growth of slip-fiber chrysotile may assume the orientation of detrital nucleus fibers along these shear zones; alternatively, early-formed authigenic cross-fiber chrysotile may have become deformed into the plane of shearing during post-depositional readjustment.

Surficial chrysotile asbestos formation elsewhere

Chrysotile asbestos occurs locally and sporadically in late veins throughout the Dun Mountain ophiolite belt (e.g., Coleman, 1966; Craw, 1979; Sinton, 1975). Some asbestos mineralization is extensive and of subeconomic significance (Williams, 1974). The veins are thought to have formed in regions of intersecting fault zones by in-filling of open fractures (Sinton, 1975) and show little or no sign of deformation. Many of the fractures formed during or after melange development and therefore, at late stages (Cretaceous–Recent) in the tectonic evolution of the ophiolite belt (Coombs *et al.*, 1976). Thus, much of the chrysotile in the ophiolite belt may have formed under surficial or near-surficial conditions, as is clearly the case in the debris flows; however geological evidence for this contention is lacking. As most natural waters derived from serpentine terrains contain appropriate amounts of Mg and Si to form serpentine (see above), chrysotile will almost certainly precipitate under appropriate Eh-pH conditions.

Much of the chrysotile in serpentinites has probably formed and may be forming today by solution of serpentine-group minerals and subsequent re-precipitation as chrysotile (as suggested by Mumpton and Thompson, 1975, for the Coalinga asbestos deposit, California) in surface or near-surface environments where reduced, alkaline conditions prevail.

ACKNOWLEDGMENTS

We are grateful to R. D. Archibald (Microbiology Department, University of Otago) for help with TEM photography, J. M. Pillidge for producing excellent thin sections of friable rubble, and Carolyn Landis for drafting. G. J. Churchman (New Zealand Soil Bureau) kindly provided DTA and IR data. The manuscript was revised and completed while one of the authors (C.A.L.) was a visiting scholar in the Department of Geosciences, University of Arizona, Tucson. Financial support was provided by the University of Otago Research Committee and Benson Memorial Fund. The manuscript has benefitted from the comments of I. Barnes, F. A. Mumpton, and an anonymous reviewer.

REFERENCES

Bain, J. A. and Morgan, D. J. (1969) The role of thermal analysis in the evaluation of impure clay deposits as mineral raw materials: *Clay Miner.* **8,** 171–192.

Barnes, I. and O'Neill, J. R. (1969) The relationships between fluids in some fresh Alpine-style ultramafics and possible serpentinization, western U.S.A: *Geol. Soc. Amer. Bull.* **80,** 1947–1960.

Barnes, I., O'Neill, J. R., and Trescases, J. J. (1978) Present day serpentinization in New Caledonia, Oman and Yugoslavia: *Geochim. Cosmochim. Acta* **42,** 144–145.

Bonatti, E., Simmons, E. C., Bregen, D., Hamlyn, P. R., and Lawrence, J. (1983) Ultramafic rock/seawater interaction in the oceanic crust: Mg-silicate (sepiolite) deposit from the Indian Ocean floor: *Earth Plan. Sci. Lett.* **62,** 229–238.

Brindley, G. W. and Brown, G. (1980) *Crystal Structures of Clay Minerals and their X-ray Identification:* Mineral. Soc., London, 495 pp.

Cashman, S. M. and Whetten, J. T. (1976) Low temperature serpentinization of periodite conglomerate on the west margin of the Chuwankum Graben, Washington: *Geol. Soc. Amer. Bull.* **87,** 1773–1776.

Chernosky, J. V., Jr. (1975) Aggregate refractive indices and unit cell parameters of synthetic serpentine in the system MgO-Al_2O_3-SiO_2-H_2O: *Amer. Mineral.* **60,** 200–208.

Cleaves, E. T., Fisher, D. W., and Bricker, O. P. (1974) Chemical weathering of serpentinite in the eastern Piedmont of Maryland: *Geol. Soc. Amer. Bull.* **85,** 437–444.

Coleman, R. G. (1966) New Zealand serpentinites and associated metasomatic rocks: *N.Z. Geol. Survey Bull.* **76,** 102 pp.

Coombs, D. S., Landis, C. A. Norris, R. J., Sinton, J. M., Borns, D. J., and Craw, D. (1976) The Dun Mountain ophiolite belt, New Zealand, its tectonic setting, constitution and origin, with special reference to the southern portion: *Amer. J. Sci.* **276,** 561–603.

Craw, D. (1979) Melanges and associated rocks, Livingstone Mountains, Southland, New Zealand: *N.Z. J. Geol. Geophys.* **22,** 443–454.

Craw, D. and Landis, C. A. (1980) Authigenic pectolite, stevensite and pyroaurite in a Quaternary debris flow, Southland, New Zealand: *J. Sed. Pet.* **50,** 497–504.

Farmer, V. C. (1974) *The Infra-red Spectra of Minerals:* Mineralogical Society, London, 559 pp.

Garrels, R. M. and Christ, C. (1965) *Solutions, Minerals and Equilibria:* Harper and Row, New York, 450 pp.

Hemley, J. J., Montoya, J. W., Christ, C., and Hostetler, P. B. (1977) Mineral equilibria in the MgO-SiO_2-H_2O system: 1. Talc-chrysotile-forsterite-brucite stability relations: *Amer. J. Sci.* **277,** 322–351.

Lahodny-Sarc, O., Dragcevic, Z., and Dosen-Sver, D. (1978) The influence of the activity of water on the phase composition of aluminum hydroxides formed by reaction of amalgamated aluminum with water: *Clays & Clay Minerals* **26,** 153–159.

Laurent, R. and Hebert, Y. (1979) Paragenesis of serpentine assemblages in harzburgite tectonite and dunite cumulate from the Quebec Appalachians: *Can. Mineral.* **17,** 857–869.

Le Bot, J. (1962) Hertzian spectroscopy of various aluminas: *Compt. Rend.* **255,** 2247–2249.

Luce, R. W. (1971) Identification of serpentine varieties by infra-red absorption: *U.S. Geol. Surv. Prof. Pap.* **750B,** 199–201.

McKellar, I. C. (1973) Te Anau-Manapouri district 1:50,000: *N.Z. Geol. Surv. Misc. Series, Map* **4,** DSIR, Wellington, New Zealand.

MacKenzie, R. C. (1970) *Differential Thermal Analysis, Volume 1:* Academic Press, London, New York, 340 pp.

Mumpton, F. A. and Thompson, C. S. (1975) Mineralogy and origin of Coalinga asbestos deposit: *Clays & Clay Minerals* **23,** 131–143.

Naumann, A. W. and Dresher, W. H. (1966) The influence of sample texture on chrysotile dehydroxylation: *Amer. Mineral.* **51,** 1200–1211.

Neal, C. and Stanger, G. (1984) Calcium and magnesium hydroxide precipitation from alkaline groundwaters in Oman, and their significance to the process of serpentinization: *Mineral. Mag.* **48,** 237–241.

Page, N. J. and Coleman, R. G. (1967) Serpentine mineral analyses and physical properties: *U.S. Geol. Surv. Prof. Pap.* **575B,** 103–107.

Papee, D., Tertian, R., and Biaish, R. (1958) Constitution of gels and crystalline hydrates of alumina: *Bull. Soc. Chim. France, ser. 5,* 1301–1310.

Postma, G. (1984) Slumps and their deposits in fan delta front and slope: *Geology* **12,** 27–30.

Sakamoto, T., Koshimuzu, H., and Shinoda, S. (1981) Hydrothermal transformation of some minerals into stevensite: in *Proc. Int. Clay Conf., Bologna, Pavia, 1981,* H. van Olphen and F. Veniale, eds., Elsevier, Amsterdam, 537–546.

Serdyuchenko, D. P. (1945) Alumino-chrysotile, a member of the isomorphous series: Serpentine-parakaolinite. *Dokl. Akad. Nauk USSR* **46,** 117–118.

Sinton, J. M. (1975) Structure, petrology and metamorphism of the Red Mountain ophiolite complex, New Zealand: Ph.D. Thesis, University of Otago, Dunedin, New Zealand, 300 pp. (unpublished).

Suggate, R. P. (1965) Late Pleistocene geology of northern part of South Island, New Zealand: *N.Z. Geol. Survey Bull.* **77,** 87 pp.

Wenner, D. B. and Taylor, H. P. (1973) Oxygen and hydrogen isotope studies of the serpentinization of ultramafic rocks in oceanic environments and continental ophiolite complexes: *Amer. J. Sci.* **273,** 207–239.

Wicks, F. J. and Plant, A. G. (1979) Electron microprobe and X-ray microbeam studies of serpentine textures: *Can. Mineral.* **17,** 785–830.

Wicks, F. J. and Whittaker, E. J. W. (1977) Serpentine textures and serpentinization: *Can. Mineral.* **15,** 459–488.

Williams, G. J. (1974) *Economic Geology of New Zealand: Australasian Institute Mining Metallurgy, Monograph* **4,** 490 pp.

Yalman, R. G., Shaw, E. R., and Colvin, J. F. (1960) The effect of pH and fluoride on the formation of aluminium oxides: *J. Phys. Chem.* **64,** 300–303.

(Received 3 September 1985; accepted 9 September 1986; Ms. 1516)